Mn *K*-edge XMCD in Mn_3MC (*M* = Zn and Ga) perovskite

Shinji Uemoto,[a] Hiroshi Maruyama,[a] Naomi Kawamura,[b] Shigeaki Uemura,[a] Naoya Kitamoto,[a] Hideki Nakao,[a] Shoji Hara,[a] Motohiro Suzuki,[c] Daniel Fruchart[d] and Hitoshi Yamazaki[a]

[a]Department of Physics, Faculty of Science, Okayama Univ., 3-1-1 Tsushima-Naka, Okayama 700-8530., Japan, [b]RIKEN, SPring-8, 1-1-1 Kouto, Mikazuki, Sayo, Hyogo 679-5148., Japan, [c]SPring-8, 1-1-1 Kouto, Mikazuki, Sayo, Hyogo 679-5198., Japan, [d]Laboratoire de Cristallographie, C.N.R.S., 166X, 38042 Grenoble, France.
Email: uemoto@mag.okayama-u.ac.jp

Mn_3MC (*M*=Zn and Ga) perovskite has attracted interest because of a variety of magnetic phase transitions. In this work, we measure temperature and magnetic field dependence of X-ray magnetic circular dichroism (XMCD) at Mn *K*-edge and discuss effect of second constituent metal on the magnetic states of Mn atoms. The spectrum in Mn_3ZnC is characterized by a dispersion-type profile. In Mn_3GaC, intensity of the positive peak at the edge is drastically reduced. The difference originates in charge transfer from Zn or Ga to Mn atoms. Temperature and magnetic field variations of the Mn *K*-edge XMCD spectrum suggest that orbital magnetic moments are closely related to the magnetic phase transition.

Keywords: X-ray magnetic circular dichroism, Mn *K*-edge, magnetic phase transition, Mn_3MC perovskite

1. Introduction

Mn_3MC (*M*=Zn and Ga) perovskite has received extensive interest due to magnetism associated with itinerant electrons (Fruchart & Bertaut, 1978; Kaneko *et al*., 1987). The magnetic property of these compounds has great variety: Those are magnetic phase transition, magnetic moments and magnetic structure. Mn atoms mainly carry the magnetic moments. Magnetic phase transition in Mn_3ZnC is classified as second-order from ferrimagnetism to ferromagnetism with increasing temperature, while that in Mn_3GaC as first-order from antiferromagnetism to ferromagnetism. The phase transitions induced by magnetic field (metamagnetism) or pressure have been also discussed from both the experimental and theoretical points of view (Kamishima *et al*., 1998). There has been, however, only a little amount of study on Mn electronic states. X-ray magnetic circular dichroism (XMCD) is a powerful tool for investigating electronic states of magnetic atoms because of element-selectivity, electron shell-specificity, and angular momentum sensitivity. XMCD at Mn *K* absorption edge is suitable for studying the phase transitions through Mn magnetic states in Mn_3MC perovskite.

We present the Mn *K*-edge XMCD spectrum in the range from 30 to 300K. In this paper, we discuss the change in Mn magnetic states caused by *M* atoms and accompanied by the magnetic phase transition. The *K*-edge originates in the $1s \rightarrow 4p$ dipole transitions, and the XMCD spectrum mainly results from 3*d* states on neighboring sites through *p*-*d* hybridization. Hence, the *K*-edge XMCD reflects magnetic polarization in the 3*d* states. Therefore, we discuss the magnetic properties from the viewpoint of Mn electronic states.

2. Experimental

The samples used in this study were powder of Mn_3ZnC and Mn_3GaC. These were prepared by solid reaction method in an evacuated quartz tube. To verify magnetic property, magnetization was measured using VSM and SQUID. In Mn_3MC (*M*=Zn and Ga) perovskite, Mn atoms occupy the face center of the cubic lattice formed by the second constituent metal *M*, and C atoms are sited at the body center of the cube. As the temperature decreased, the second-order transition in Mn_3ZnC occurs at T_t=233K with a tetragonal distortion. Below T_t, the magnetic unit-cell is formed of four Mn layers: Two canted-ferromagnetic layers and two ferromagnetic layers. Since Mn_3GaC is antiferromagnetic at low temperatures, an abrupt increase of magnetization happens at T_t=170K due to the first-order transition accompanied with decrease in volume. Curie Temperature (T_c) is about 260K.

Mn *K*-edge XMCD and XANES spectra were measured in transmission mode by the helicity-modulation (HM) method (Suzuki *et al*., 1998) on BL39XU at SPring-8. Although the *K*-edge XMCD generally shows very small signal and a complicated profile, the HM method can provide the spectrum improved in statistical accuracy and resolution. Magnetic field was applied antiparallel to the direction of the incident X-ray. XMCD ($\Delta\mu t$) and XANES (μt) are defined as $\Delta\mu t = \mu_+ t - \mu_- t$ and $\mu t = [\mu_+ t + \mu_- t]/2$, where $\mu_+ t$ and $\mu_- t$ are absorption for $+\hbar$ and $-\hbar$ helicity of incident photons, respectively. XMCD ($\Delta\mu t$) can be expressed as follows:

$$\Delta\mu t \propto P_C \cdot \sigma \cdot \cos\theta \cdot \Delta\rho/\rho, \qquad (1)$$

where σ represents magnetization, θ the angle between the sample magnetization and the incident X-ray wave vector. $\rho = \rho(\uparrow) + \rho(\downarrow)$ and $\Delta\rho = \rho(\uparrow) - \rho(\downarrow)$ are represented by the density of states up-spin $\rho(\uparrow)$ and $\rho(\downarrow)$ bands. XMCD spectrum is normalized by the edge jump in XANES spectrum. Absorption edge energy E_0 was determined as the first inflection point of the XANES spectrum. Temperature dependence of XMCD spectrum was carried out in the temperature range from 30 up to 300K in heating process under 0.6T. The magnetic field is enough to saturate magnetically the samples except for Mn_3ZnC in ferrimagnetic states. The magnetic field dependence of XMCD spectrum was measured using a superconducting magnet up to 7T.

3. Results and Discussion

3.1 Effect of M atoms on Mn atoms

The Mn *K*-edge XMCD and XANES spectra are shown in Fig.1. The spectra in Mn_3ZnC at 240K and Mn_3GaC at 200K are denoted by closed circle and open triangle, respectively, in ferromagnetic phase. The XANES spectra indicate that these compounds are metallic. The dichroic signal is observed around E_0 with intensity of the order of 10^{-3} to XANES spectrum. In Mn_3ZnC, the XMCD spectrum is characterized by a dispersion-type profile having a positive peak just on the edge and a negative one at 3 eV above, which is very similar to Fe *K*-edge XMCD in pure Fe (Maruyama *et al*., 1991). This suggests that Mn 3*d* states in Mn_3ZnC resemble the electronic structure of Fe atoms. On the other hand, in Mn_3GaC the positive peak intensity is drastically reduced, whereas the negative one is enhanced. The negative peaks (at 2 and 7eV) are similar to the profile observed in

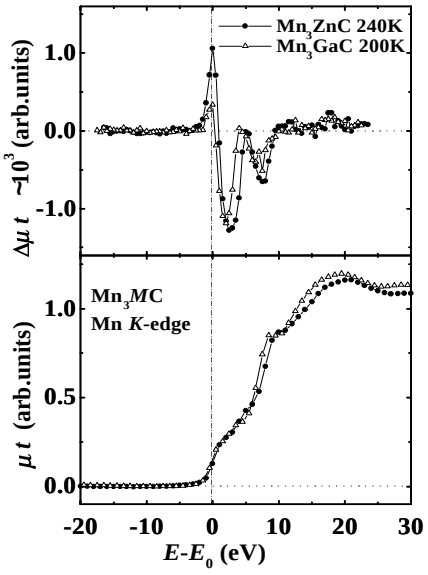

Figure 1
Mn *K*-edge XANES (lower panel) and XMCD (upper panel) spectra in Mn_3MC. The spectra in Mn_3ZnC at 240K and Mn_3GaC at 200K are denoted by closed circle and open triangle, respectively. The vertical line displays the absorption edge.

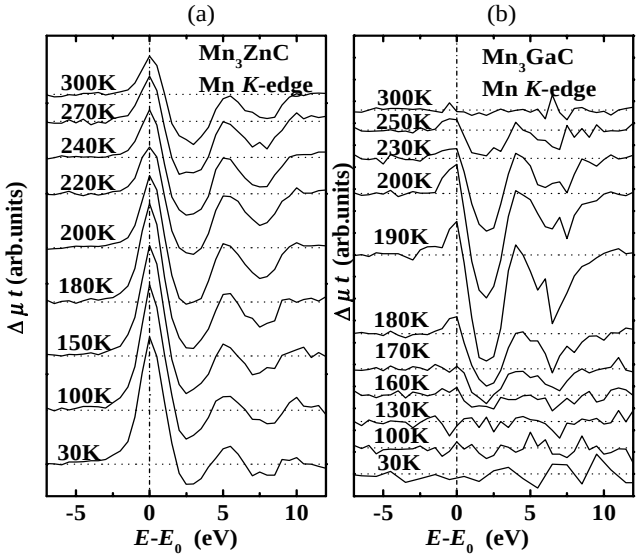

Figure 2
Temperature dependence of Mn *K*-edge XMCD spectra, (a) in Mn_3ZnC and (b) in Mn_3GaC, in the range from30 (bottom) to 300K (top).

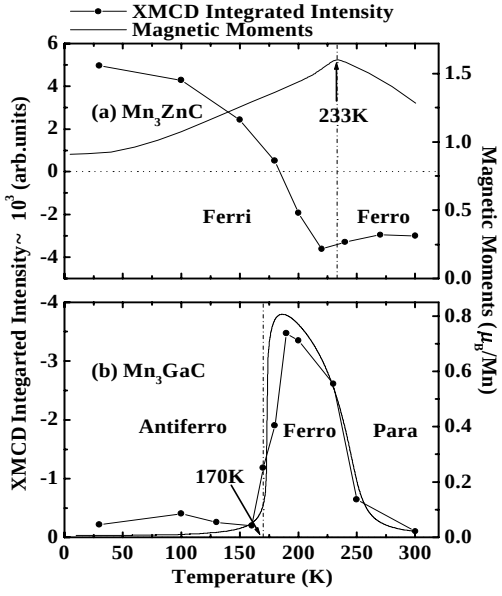

Figure 3
Temperature-dependent integrated intensity of XMCD, (a) in Mn_3ZnC and (b) in Mn_3GaC, in comparison with the temperature variation of magnetic moments. The vertical line displays the transition temperature T_t

Mn_3ZnC. The positive peak strongly reduced may be related to a decrease of spin polarization in the 3*d*-states. We consider that the difference between Mn_3ZnC and Mn_3GaC originates in charge transfer from Zn or Ga to Mn atoms. This is interpreted as a decrease of Mn *p* (3*d*) up-spin hole by changing from Zn to Ga. According to the magneto-optical sum rule for the *K*-edge (Igarashi & Hirai, 1994), the integrated intensity could be connected with expectation value of orbital angular momentum par Mn 4*p* hole. The present results indicate that orbital moment of *p* conduction bands is not quenched. Order of the orbital moment is estimated to be $10^{-3}\mu_B$ par Mn atom.

3.2 Temperature dependence of XMCD

Figure 2 shows temperature dependence of XMCD spectrum, (a) in Mn_3ZnC and (b) in Mn_3GaC, in the range from 30 to 300K. In Mn_3ZnC, the temperature dependence of positive peak (at 0eV) markedly differs from those of two negative peaks (at 3 and 8eV). In ferrimagnetic phase below T_t=233K, the positive peak intensity increases with decreasing temperature, although the magnetization decreases. On the other hand, the negative peaks normally show a decrease in intensity as well as the change in magnetization due to the second-order transition. In ferromagnetic phase ranging from 233 up to 300K, both the positive and negative XMCD signals become relatively small. As the temperature is decreased from 300K, the positive peak intensity first increases monotonically and then rapidly after crossing over the transition temperature, while the negative peak is gradually reduced its amplitude. Consequently, XMCD integrated intensity shows a peculiar behaviour in the temperature dependence, as shown in Fig.3 (a), compared with the variation of average magnetic moments. The integration was made over the range of $-5\text{eV}<(E-E_0)<+13\text{eV}$. The integrated intensity first maintains a negative value in ferromagnetic phase and turns into decrease around T_t, which happens almost with the appearance of cusp in magnetization. As the temperature is decreased further, the integrated intensity changes a sign from negative to positive around 185K; the positive contribution overcomes the negative component at lower temperatures. This behaviour is explained as follows: the observed spectrum is an average of three Mn sites, and the negative contribution originates in ferromagnetic phase, so that the positive component results from the appearance of the canted-ferromagnetic layers in ferrimagnetic phase. According to the sum rule, the present results indicate that the orbital angular momentum of Mn 4*p* unoccupied bands changes a sign from negative to positive. Moreover, below 185K the 4*p* bands have the orbital moment being antiparallel to the 3*d* spin magnetic moments.

In Mn_3GaC, no signal of XMCD spectrum is observed because of antiferromagnetism below T_t (170K). As the temperature is increased, an abrupt increase occurs in the XMCD signal around T_t due to the first-order transition. The spectrum

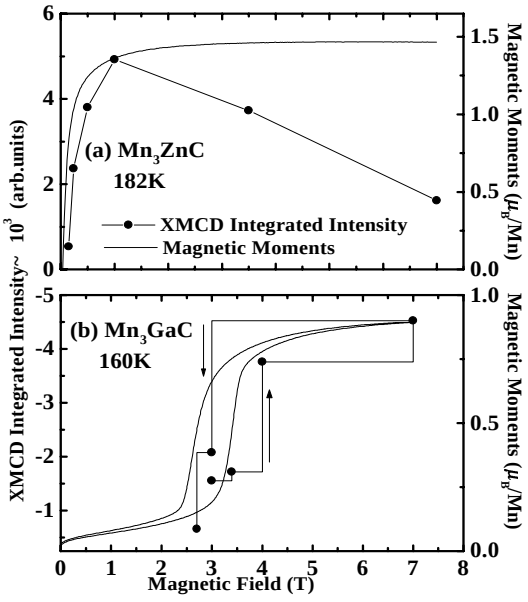

Figure 4
Magnetic field-dependent integrated intensity of XMCD, (a) in Mn_3ZnC and (b) in Mn_3GaC, in comparison with the magnetic field variation of magnetic moments.

sensitively reflects change in the density of states in the vicinity of the Fermi level, so that the XMCD intensity directly corresponds to bulk magnetization. In ferromagnetic phase, the intensity decreases monotonically as the temperature increases. No spectral features are significantly observed in paramagnetic phase above T_c. The temperature dependence of the integrated intensity is in good agreement with the variation of the average magnetic moments (Fig.3 (b)). These results indicate that the orbital moments exhibit the similar temperature dependence to the bulk magnetization in Mn_3GaC having collinear spin structure.

3.3 Field dependence of XMCD

Magnetic field dependence of XMCD spectrum in Mn_3ZnC at 182K and Mn_3GaC at 160K was measured up to 7T. In Mn_3ZnC, the XMCD signal increases with increasing the magnetic field, however the increase rate of the negative peak intensity is larger than that of the positive one. Hence, the negative contribution becomes relatively large with increasing magnetic field. Indeed, the integrated intensity gradually decrease with increasing magnetic field in the range above 1T, in contrast with the monotonical increase of magnetic moment, as shown in Fig.4 (a). In this case, the XMCD intensity does not hold eq. (1). This result indicates that high magnetic fields *suppress* the orbital moment of Mn *p* unoccupied bands in spite of the increase of average magnetic moments. This peculiar behavior corresponds with those in the temperature dependence. We interpret this phenomenon as a process which the canted-moments are aligned by high magnetic field or temperature.

In Mn_3GaC, the metamagnetic transition takes place around 3.5T with increasing field at 160K. We observed an abrupt increase of the XMCD signal and field hysteresis due to the first-order transition. In contrast with Mn_3ZnC, the integrated intensity keeps a negative sign and its absolute value normally increases with increasing the magnetic moment (Fig.4 (b)). This result indicates that the orbital moment is promoted by the magnetic field. It may be explained as an increase of ferromagnetic component in spin-flip states. Consequently, the field dependence of XMCD intensity shows a different behavior between Mn_3GaC and Mn_3ZnC. We consider that this originates in the different spin structure being non-collinear in Mn_3ZnC and collinear in Mn_3GaC.

4. Conclusion

We have measured the dependence of XMCD spectrum on temperature and magnetic field at Mn *K*-edge in Mn_3MC (*M*=Zn and Ga). The XMCD spectrum shows several differences between Mn_3ZnC and Mn_3GaC. The difference in spectral profile originates in charge transfer from Zn or Ga to Mn atoms. The peculiar temperature and magnetic field dependence observed in Mn_3ZnC suggests that the orbital moments of Mn *p* bands be closely related to the appearance of canted-ferromagnetic structure. In Mn_3GaC, we have observed an abrupt change in the XMCD intensity accompanied with the first-order transition induced by temperature and magnetic field. The present result is the first observation that orbital moment is associated with magnetic phase transition in Mn_3MC perovskite.

The authors express their thanks Professor M. Shirai for many useful discussions. This work has been carried out under the approval of SPring-8 PRC (Nos. 1999A0173, 1999B0385 and 2000A0383).

References

Fruchart, D. & Bertaut, E. F. (1978) *J. Phys. Soc. Jpn.* **44**(3) 781-791
Igarashi, J. & Hirai, K. (1994). *Phys. Rev.* **B50**(24), 17820-17829
Kamishima, K., Bartashevich, M I., Goto, T., Kikuchi, M. & Kanomata, T. (1998) *J. Phys. Soc. Jpn.* **67**(5) 1748-1754
Kaneko, T., Kanomata, T., & Shirakawa, K. (1987) *J. Phys. Soc. Jpn.* **56**(11) 4047-4055
Maruyama, H., Iwazumi, T., Kawata, H., Koizumi, A., Fujita, M., Sakurai, H., Itoh, F., Namikawa, K., Yamazaki, H. & Ando, M. (1991) *J. Phys. Soc. Jpn.* **60**(5) 1456-1459
Suzuki, M., Kawamura, N., Mizumaki, M. Urata, A., Maruyama, H., Goto, S. & Ishikawa, T. (1998). *Jpn. J. Appl. Phys.* **37**, L1488-L1490

 Received 31 July 2000 • Accepted 9 November 2000